Biosensors and Bioelectronics 65 (2015) 281–286

Contents lists available at ScienceDirect

Biosensors and Bioelectronics

journal homepage: www.elsevier.com/locate/bios

Three-dimensional electrochemical immunosensor for sensitive detection of carcinoembryonic antigen based on monolithic and macroporous graphene foam

Jiyang Liu [a,b], Jiao Wang [a], Tianshu Wang [b,c], Dan Li [b], Fengna Xi [a,*], Jin Wang [b,c,d,**], Erkang Wang [b,**]

[a] Department of Chemistry, Zhejiang Sci-Tech University, Hangzhou, Zhejiang 310018, China
[b] State Key Laboratory of Electroanalytical Chemistry, Changchun Institute of Applied Chemistry, Chinese Academy of Sciences, Changchun, Jilin 130022, China
[c] College of Physics, Jilin University, Changchun, Jilin 130012, China
[d] Department of Chemistry, Physics and Applied Mathematics, State University of New York at Stony Brook, Stony Brook, NY 11794-3400, USA

ARTICLE INFO

Article history:
Received 20 August 2014
Received in revised form
6 October 2014
Accepted 7 October 2014
Available online 16 October 2014

Keywords:
3D graphene
Electrochemical immunosensors
Carcinoembryonic antigen
Lectin
Horseradish peroxidase-labeled antibody
Lectin–sugarprotein interaction

ABSTRACT

A high performance three-dimensional (3D) electrochemical immunosensor was developed for sensitive detection of the tumor biomarker, carcinoembryonic antigen (CEA). Monolithic and macroporous graphene foam grown by chemical vapor deposition (CVD) served as the scaffold of the free-standing 3D electrode. Immuno-recognition interface was fabricated via simple and non-covalent immobilization of antibody using lectin-mediated strategy. Briefly, the well-known lectin macromolecule (*concanavalin A*, Con A) monolayer was functionalized on 3D graphene (3D-G) using in-situ polymerized polydopamine as the linker. Then the widely used horseradish peroxidase (HRP)-labeled antibody (anti-CEA) in immunoassays was efficiently immobilized to demonstrate the recognition interface via the biospecific affinity of lectin with sugarprotein. The 3D immunosensor is able to detect CEA with a wide linear range (0.1–750.0 ng ml^{-1}), low detection limit (~90 pg ml^{-1} at a signal-to-noise ratio of 3), and short incubation time (30 min). Furthermore, this biosensor was used for the detection of the CEA level in real serum samples.

1. Introduction

Early clinical diagnosis of cancer is the key to a higher survival rate. Tumor markers are macromolecules existing in tumor cells or host body fluids, which are produced by tumors associated with cancers. It has been proven that sensitive detection of tumor markers is of great significance in early detection and monitoring recurrence of cancers (Kitano, 2002; Srinivas et al., 2001). Till now, numerous immunoassays for tumor marker have been developed (e.g., enzyme-linked immuno-sorbent assay (ELISA) (Voller et al., 1978; Yates et al., 1999), chemiluminescence (Fu et al., 2006, 2008), and mass spectrometric immunoassays (Niederkofler et al., 2001; Hu et al., 2007)). Among those different techniques, electrochemical immunosensors have received a particular attention because of their simple instrumentation, fast response time, and portability (Tang et al., 2011; Guo et al., 2011; Luo et al., 2014; Kanso et al., 2014). Current electrochemical immunosensors, however, are often limited by complex detection scheme, poor sensitivity and stability, and long detection time. For instance, many immunosensors rely on two or three protocols for signal amplification to improve sensitivity (Du et al., 2011; Begard et al., 2014). The antibodies immobilized via covalent reaction, nanomaterial adsorption or polymer entrapment may compromise the detection efficiency due to low activity or poor long-term stability. In addition, the incubation time might be long due to low diffusion of macromolecules.

Over the past few years, it has been proven that electrode material and architecture play critical roles to achieve a simple, sensitive and stable detection in protein-based bioanalysis (Zhang et al., 2011; Ojeda et al., 2014). The applications of three dimensional (3D) macroporous electrodes are highly desirable since they can improve the performance of electrochemical sensors (Wang et al., 2014; Si et al., 2013; Yang et al., 2013; Dong et al., 2012a). For instance, the large internal surface and macroporous morphology improve the density, accessibility as well as the stability of the

* Corresponding author. Fax: +86 571 86843653.
** Corresponding authors at: Chinese Academy of Sciences, Changchun Institute of Applied Chemistry, State Key Laboratory of Electroanalytical Chemistry, Changchun, Jilin 130022, China. Fax: +86 431 85689711.
E-mail addresses: fengnaxi@zstu.edu.cn (F. Xi), jin.wang.1@stonybrook.edu (J. Wang), ekwang@ciac.jl.cn (E. Wang).

http://dx.doi.org/10.1016/j.bios.2014.10.016
0956-5663/

bioactive affinity ligands (e.g. antigen or antibody). In addition, interconnected open porosity of the host 3D electrode facilitates the kinetic diffusion and mass transfer of macromolecules (Xi et al., 2013). Among those significant progress made in building 3D electrode, the fabrication of macroporous Au electrodes was dominated. Current 3D macroporous Au electrodes, however, were mainly prepared by precisely controlled electrochemistry process (Patel et al., 2013). As the morphology of the resulting 3D Au film was difficultly controllable, the electrode was easily irreproducible. Due to its fascinating electronic and chemical properties, graphene exhibited immense potential for the development of novel and ultra-sensitive electrochemical biosensors (Liu et al., 2012; Wang et al., 2012; Feng et al., 2011). Recently, 3D monolith of graphene foam with unique macroporous structure has been grown via CVD (Chen et al., 2011). Compared with the conventional 2D (planar) electrochemical electrodes, such 3D graphene (3D-G) electrodes are attractive for the construction of ultrasensitive chemical sensors due to the unique advantages of macroporous scaffold, large active surface area, unhindered substance diffusion, high conductivity and stability (Xi et al., 2013; Liu et al., 2012; Dong et al., 2012b, Huang et al., 2010). More importantly, 3D-G electrodes provide potential for cheap and large-scale preparation with high reproducibility. As so far, few biosensors are developed based on 3D-G foam grown by CVD. This is mainly because the 3D-G foam is free-defectable and exhibits ultrahigh hydrophobicity, which imposes difficulties in its biological functionalization and application. It is well known that amphipathic polydopamine (pDA) formed by in-situ polymerization of dopamine in alkaline condition is able to adhere well onto a wide range of hydrophobic or hydrophilic surfaces (Lee et al., 2007; Morris et al., 2009). Additionally, pDA provides abundant reactive handles that can conjugate with a wide spectrum of thiol- or amine-containing molecules (e.g., protein) via Michael addition or Schiff base reactions (Cheng et al., 2013; Morris et al., 2009). Therefore, the biofunctionalization of 3D-G via pDA as the universal linker might open up the possibilities to develop new platform for three-dimensional electrochemical biosensing.

In the present work, a novel three-dimensional electrochemical immunosensor with high performance is developed using 3D-G foam as a monolithic and macroporous carbon electrode. Sensitive detection of the tumor biomarker, carcinoembryonic antigen (CEA), is achieved via immuno-recognition interface immobilized on lectin monolayer. Briefly, 3D-G electrode was firstly functionalized with a well-known lectin, *concanavalin A* (Con A) using in-situ polymerized polydopamine as the linker. Then, the immunosensing interface is efficiently fabricated by immobilizing HRP-labeled anti-CEA antibody (HRP-Ab) via biospecific lectin–sugarprotein interaction. The detection lies in the signal changes of the solution-phase redox probe in differential pulse voltammetry (DPV) after the capture of CEA to the anti-CEA interface. Owing to the 3D architecture, extraordinary properties of graphene and indirect antibody immobilization, the immunosensor demonstrates outstanding performance in terms of detection range, sensitivity, response time, and stability even no complex strategy for signal amplication is used.

2. Experimental

2.1. Reagents and apparatus

Dopamine hydrochloride (98%), bovine serum albumin (BSA) and *concanavalin A* (Con A) from *canavalia ensiformis* (Jack Bean) were purchased from Sigma-Aldrich (USA). Horseradish peroxidase (HRP) (E.C.1.11.1.7, 250 U mg^{-1}) was purchased from Shanghai Sanjie Biotechnology Co., Ltd (Shanghai, China). Carcinoembryonic antigen (CEA), HRP labeled anti-CEA antibody (HRP-Ab) and prostate specific antigen (PSA) were purchased from Keyuezhongkai Biotech Co., Ltd. (Beijing, China) and were stored at 4 °C before use. β-D-(+)-Glucose was purchased from Beijing Chemical Reagent (Beijing, China). All other chemicals were of analytical grade and used without further purification. All aqueous solutions were prepared by using ultrapure water (18.2 MΩ cm^{-1}) from a Milli-Q Plus system (Millipore).

Scanning electron microscopy (SEM) images were obtained at 5.0 kV on a JSM-6700F (JOEL, Japanese) field emission scanning electron microscope. Static contact angles were measured on a drop shape analysis system G10/DSA10 contact angle system. Electrochemical measurements were performed on a CHI 660D electrochemical analyzer (Shanghai CH Instrument Company, China).

2.2. Preparation of 3D-G based immunosensor and the biosensing process

As previously described (Xi et al., 2013), 3D graphene foam was synthesized by CVD with nickel foam being the growth substrate. After growth, the nickel substrate was removed by incubation with 3 M HCl at 80 °C for 12 h. The freestanding 3D-G foam (0.5 cm × 0.5 cm, 1 mm thick) was then fixed onto a glass slide. The electrical lead was made by silver paint and copper wire insulated with silicone rubber. Similar to the work previously reported (Lee et al., 2007; Morris et al., 2009), polydopamine (pDA) was then coated onto a 3D-G electrode by immersing this electrode into a dopamine monomers solution (1 mg ml^{-1} in 0.05 M PBS solution, pH 8.5) for 30 min. After rinsing away the unbound pDA, the 3D-G/pDA electrode was immersed into a *concanavalin A* (Con A) solution (0.5 mg ml^{-1} in 10 mM PBS containing 1 mM $CaCl_2$ and 1 mM $MnCl_2$, pH 7.5) for 40 min, followed by removing non-specifically adsorbed Con A via thorough rinse. Afterwards, the 3D-G/pDA/Con A electrode was dipped in a HRP-labeled anti-CEA antibody solution (HRP-Ab, 100 μg ml^{-1}) for 1 h. By this step, anti-CEA antibody was captured on Con A to demonstrate CEA recognition interface through the biospecific interaction between Con A and HRP. Then the modified electrode was dipped into an HRP solution (1.0 mg ml^{-1} in 10 mM PBS, pH 7.5) for 1 h to block the free sites of both Con A and the modified materials. After rinsing with distilled water, the obtained immunosensor (3D-G/pDA/Con A/HRP-Ab) was stocked in PBS (0.05 M, pH 7.0) at 4 °C before use.

For the biosensing of CEA, the immunosensors were incubated with various concentrations of CEA antigen (Ag) at 25 °C. After forming antigen–antibody complex, the detection was performed by measuring the inhibited current of $Fe(CN)_6^{3-/4-}$ using differential pulse voltammetry (DPV). The ratio of I/I_0 was evaluated, where I_0 represented the blank peak current, and I represented the current after each detection. To investigate the selectivity of the fabricated immunosensor, interference study was performed using bovine serum albumin (BSA), prostate specific antigen (PSA), horseradish peroxidase (HRP) and glucose. A 3.0 ng ml^{-1} of CEA solution containing 30.0 ng ml^{-1} of interfering substances was measured by the immunosensor using the above sensing protocol.

2.3. Electrochemical measurements

Electrochemical measurements were performed on a CHI 660D electrochemical analyzer (Shanghai CH Instruments, China). A conventional three-electrode system was used consisting of a bare or modified 3D-G working electrode, an Ag/AgCl (saturated with KCl) reference electrode, and a platinum disk auxiliary electrode. The solution of $K_3Fe(CN)_6/K_4Fe(CN)_6$ (1:1, 1.0 mM containing 0.1 M KCl) was used as the supporting electrolyte for all electrochemical

measurements. Cyclic voltammetric experiments were carried out with the scan rate of 100 mV/s. Electrochemical impedance spectroscopy (EIS) investigation was performed with the frequencies ranging from 10^4 to 10^{-1} Hz. DPV was performed by scanning from 0.4 V to 0.05 V (modulation time: 50 ms, interval time: 0.5 s, step potential: 5 mV, modulation amplitude: 50 mV).

3. Results and discussion

3.1. Fabrication of immunosensing interface on 3D-G electrode

Fig. 1 shows a schematic illustration of the fabrication of the immunosensor. Effective immobilization of affinity antibody on biocompatible electrode material is crucial to achieve highly sensitive detection. As the graphene foam is highly hydrophobic, the improvement of the hydrophilicity of graphene foam is crucial for biomolecules loading and bioactivity preserving in bioanalysis. In this work, polydopamine (pDA) was coated onto 3D-G via in-situ polymerization of dopamine in alkaline condition to render the electrode hydrophilic and to serve as a powerful linker to covalently immobilize *concanavalin A* (Con A), one of carbohydrate-binding lectin proteins. It has been proven that the ambiphilic pDA forms strong bonds with various hydrophobic or hydrophilic surfaces through their ortho-dihydroxy-phenyl functional groups (Lee et al., 2007; Morris et al., 2009). In addition, pDA acts as a cross-linking platform for further covalent immobilization of other chemical/biological molecules (thiol- or amine-containing molecules, e.g. protein) via Michael addition or Schiff base reactions. After that, immunosensing interface to anchor CEA was fabricated onto lectin modified electrode by recognition specificities between Con A and sugarprotein conjugated antibody (HRP-Ab). Biospecific affinity between Con A and sugar chains intrinsically located on the surface of HRP is reliable and has been successfully applied for the fabrication of layer-by-layer multilayers (Xi et al., 2011). One Con A molecule could bind with four HRP structures. It is well known that the antibody immobilization plays a key role for the performance of immunosensors in there selectivity, sensitivity and stability. Compared with other antibody immobilization protocols (e.g. covalent immobilization, nanomaterial adsorption or polymer entrapment), this antibody immobilization mediated by lectin–sugarprotein interaction offers an indirect and oriented immobilization on biocompatible matrix. Combined with the macroporous morphology of 3D-G, antibodies could be immobilized onto the 3D electrode to provide high activity, excellent recognition ability and stability. After the capture of CEA to the immobilized anti-CEA, the detection lies in the signal changes of the solution-phase redox probes ($[Fe(CN)_6]^{4-/3-}$) measured by differential pulse voltammetry (DPV).

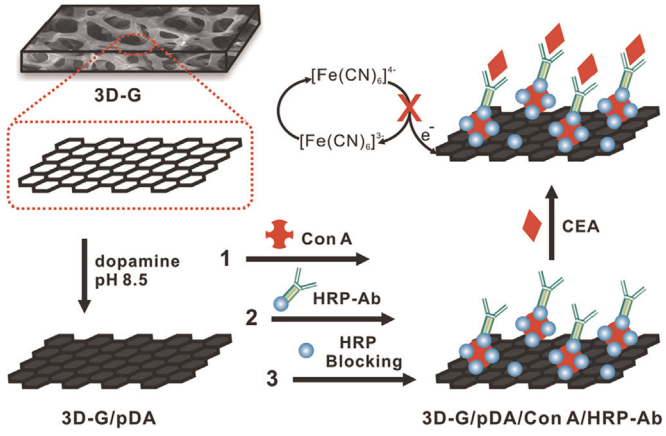

Fig. 1. Schematic illustration of the fabrication and CEA detection process of the immunosensor.

3.2. Characterization of immunosensing interface

SEM and contact angle experiments were carried out to characterize the modification of 3D-G electrode. Fig. 2A shows typical SEM images of CVD-grown 3D-G at different magnifications. Obviously, 3D-G foam exhibits a monolithic and well-defined macroporous structure. And the surface of graphene skeleton has numerous wrinkles and ripples. The unique architecture could greatly accelerate the rate of diffusion and mass transfer of ion and macromolecular. For comparison, a much rough surface was achieved after pDA coating (Fig. 2B). As shown in Fig. 2C and D, the contact angles of bare 3D-G and 3D-G/pDA were 127.8° and 82.2°, respectively. Obviously, 3D-G/pDA showed lower contact angle and better hydrophilicity. Therefore, 3D-G/pDA could provide a biocompatible and macroporous surface to improve the density, accessibility and stability of the bioactive antibodies, which was beneficial to the following fabrication of immunosensor.

CVs at each fabrication process with $[Fe(CN)_6]^{4-/3-}$ as probes were recorded and shown in Fig. 3. The freestanding 3D-G electrode was used as the base electrode. Owing to its 3D architecture and exceptional properties, the 3D-G electrode presents a high redox peak current density of $[Fe(CN)_6]^{4-/3-}$ (Fig. 3, curve a), which is almost three times larger than that from the conventional planar glassy carbon (GC) electrode (inset of Fig. 3), suggesting the potential of 3D-G electrode for highly sensitive electrochemical detection. For comparison, 3D-G/pDA exhibited an increased peak current due to its improved hydrophilicity (Fig. 3, curve b). When Con A and HRP-Ab were successfully adsorbed onto the electrode, there was an obvious decrease of the current (Fig. 3, curve c, d), which suggested the efficient immobilization. The reason for the decrease of current is that the movement of $[Fe(CN)_6]^{4-/3-}$ towards the electrode surface is hindered by Con A and HRP-Ab proteins. Finally, HRP was used to eliminate the remaining binding site of Con A and a decrease of current was also obtained (Fig. 3, curve e).

Electrochemical impedance spectroscopy (EIS) was also conducted to investigate the electron transfer properties of the obtained electrodes after each modification stage. The electron-transfer resistance (R_{ct}) relates to the diameter of the semicircle of the impedance curve. As shown in Fig. 4A, the electron transfer resistance of the bare 3D-G and 3D-G/pDA is about 113.8 (Fig. 4A, curve a) and 76.5 Ω (Fig. 4A, curve b), respectively. The low R_{ct} of the 3D-G/pDA electrode may be attributed to the large active surface area offered by the graphene foam and the improved hydrophilicity. However, the successive immobilization of Con A and HRP-Ab on the electrode surface significantly change the interfacial electron transfer. The R_{ct} of Con A modified electrode (3D-G/pDA/Con A) is estimated to be 970.2 Ω (Fig. 4B, curve c). After HRP-Ab coupling, R_{ct} for antibody modified electrode is found to be 2442.5 Ω (Fig. 4B, curve d), and that of HRP-blocked immunoelectrode (3D-G/pDA/Con A/HRP-Ab/HRP) is 3123.4 Ω (Fig. 4B, curve e). The reason is that the insulating protein layers on the electrode of Con A, HRP-Ab and the blocking HRP hinder the electron transfer and decrease the accessibility of electrochemical probe. Lastly, the modified electrode was incubated with CEA which is the specific target of the immobilized anti-CEA. Hence, it binds specially to anti-CEA and this result in a further increase in impedance due to the additional steric hindrance caused by the bulky CEA protein molecules.

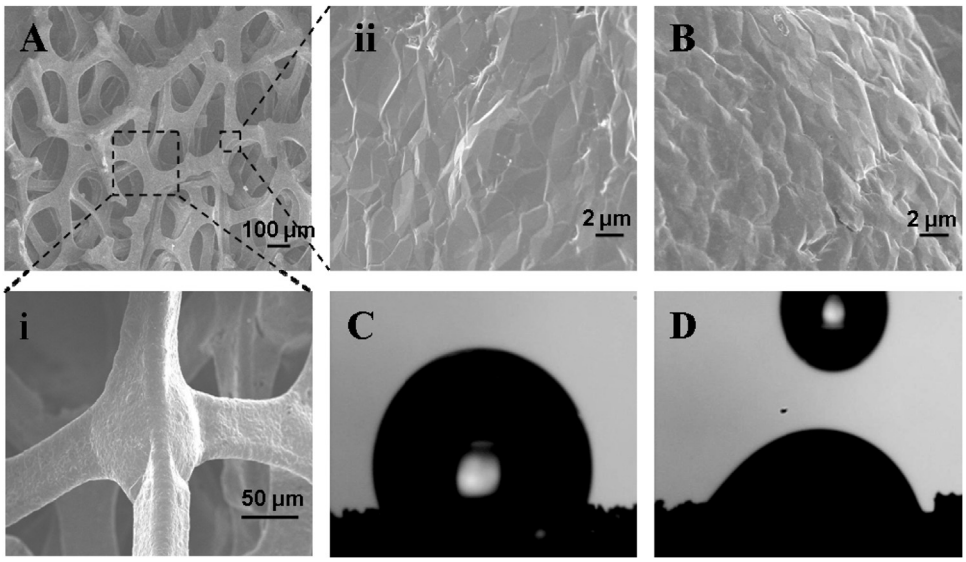

Fig. 2. (A) SEM images of the CVD-grown 3D-G with different magnification (i and ii). (B) SEM image of 3D-G/pDA. (C and D) Contact angle images of 3D-G (C) and 3D-G/pDA (D).

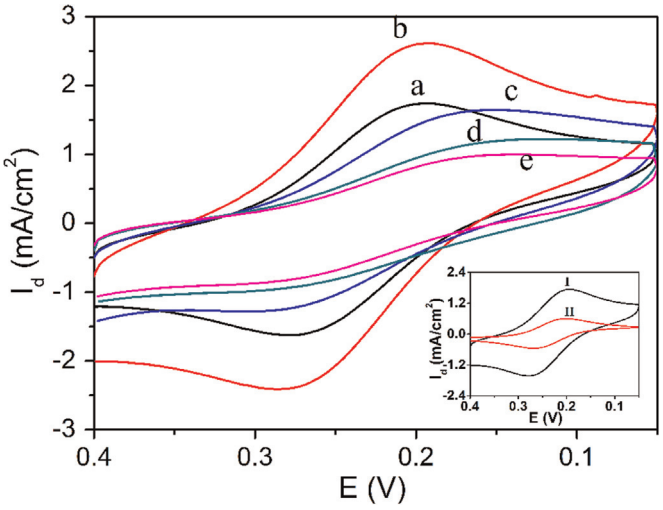

Fig. 3. Cyclic voltammograms (CVs) of different modified electrodes measured in 1.0 mM $[Fe(CN)_6]^{4-/3-}$ containing 0.1 M KCl (a) 3D-G, (b) 3D-G/pDA, (c) 3D-G/pDA/Con A, (d) 3D-G/pDA/Con A/HRP-Ab without HRP blocking, (e) 3D-G/pDA/Con A/HRP-Ab with HRP blocking (the final immunoelectrode). Inset was the CVs of 3D-G (i) and GC (ii) in 1.0 mM $[Fe(CN)_6]^{4-/3-}$ containing 0.1 M KCl.

3.3. Detection of CEA with the developed immunosensor

Carcinoembryonic antigen (CEA) is a glycoprotein most often associated with colorectal carcinomas and commonly used as a clinical marker of tumors for clinical diagnosis of colorectal, pancreatic, gastric, and cervical carcinomas (Cai et al., 2012). The analytical protocol illustrated in Fig. 1 was employed in this study. The detection lies in the current changes of $[Fe(CN)_6]^{4-/3-}$ after the attachment of CEA to the immobilized anti-CEA measured by differential pulse voltammetry (DPV). To determine the optimum incubation time for CEA detection, the kinetic experiment was done and the results were shown in Fig. 5. The DPV peak current of the fabricated immunsensor decreased significantly with increasing the incubation time in 1.0 ng ml^{-1} of CEA solution, and reached a plateau at about 30 min. Thus, the optimum interaction time was considered as 30 min. 3D-G possesses unhindered substance/ion diffusion throughout the macroporous structure and shortens the binding time of macromolecules.

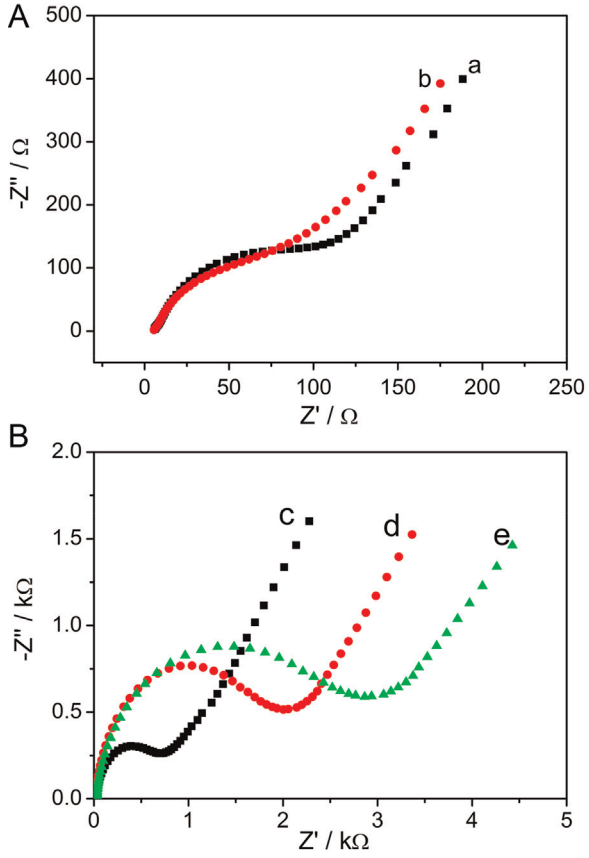

Fig. 4. EIS of different modified electrodes measured in 1.0 mM $[Fe(CN)_6]^{4-/3-}$ containing 0.1 M KCl: (a) 3D-G, (b) 3D-G/pDA, (c) 3D-G/pDA/Con A, (d) 3D-G/pDA/Con A/HRP-Ab without HRP blocking, (e) 3D-G/pDA/Con A/HRP-Ab with HRP blocking (the final immunoelectrode).

With a frequently used electrochemical probe ($[Fe(CN)_6]^{4-/3-}$) as the signal tag, DPV is used for electrochemical detection of CEA. As a well-known pulse technique without the influence of the charging current of electric double layer, DPV is very sensitive to signal change with low magnitude (Liu et al., 2013). In addition, it is a fast detection method and the corresponding detection could

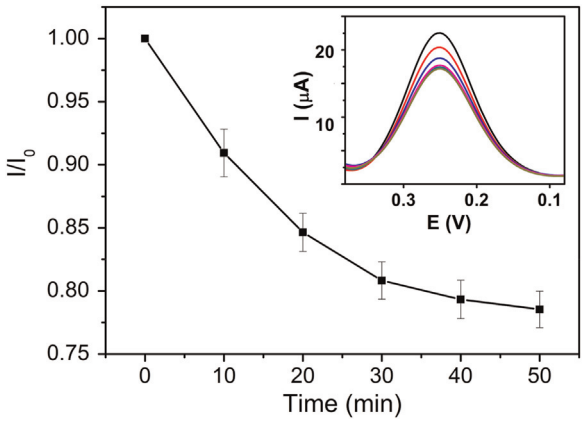

Fig. 5. The time-dependent DPV signal response for CEA detection. I/I_0: I represented the peak current of the sensor after each detection, and I_0 represented the blank peak current. Error bar=RSD (n=3). Inset is the DPV responses of the immunosensor after being incubated with CEA (1.0 ng ml^{-1}) for 0, 10, 20, 30, 45, 60 min (from up to bottom).

be finished within one minute. The DPV current responses were measured by changing the CEA concentration and the results were shown in Fig. 6A. As seen, the decrease of DPV peak current signals was directly related to the increase of CEA, because the antigen–antibody complex coating on the surface of the electrode inhibited the electron-transfer. In Fig. 6B, I/I_0 was used to evaluate the DPV peak current response to CEA. There was a linear relationship between I/I_0 and logarithmic CEA concentration from 0.1 to 750.0 ng ml^{-1} (R^2=0.9924). Meanwhile, the immunosensor had an extrapolated lower detection limit of ~90 pg mL^{-1} (at a signal-to-noise ratio of 3). In contrast, comparative studies were carried out using the GC as the base electrode. Due to the limited electrode surface area and the high suppression of electron-transfer caused by three proteins layers, the signal of $[Fe(CN)_6]^{4-/3-}$ on the immunoelectrode was small. A narrow linear range (8.0 to 120.0 ng mL^{-1}) was obtained. Compared with the conventional planar electrode system, 3D-G based immunoassay is obviously sensitive. The detection limit obtained by the 3D immunoassay system was lower than those based on Au nanoparticles (AuNPs)/carbon nanotube (CNT)-chitosan (CS) system (Huang et al., 2010; Gao et al., 2011a), AuNPs/Fe_3O_4-CS/prussian blue (Chen et al., 2010), CNT-Au nanoclusters (Gao et al., 2011b), and graphene-magnetic bead-enzyme-labeled antibody-AuNPs bioconjugate (Jin et al., 2014). It was noting that the proposed 3D electrochemical immunoassay was simple without complex strategy for signal amplification to improve sensitivity. The outstanding performance could be attributed to the high electrical conductivity and unhindered substance diffusion provided by the 3D-G. In addition, the macroporous scaffold and large active surface area of 3D electrode increase the amount of immobilized antibody on the recognition interface.

3.4. Selectivity, stability, and reproducibility of the developed immunosensor

To evaluate the reproducibility of the fabricated immunosensors, five electrodes were prepared. The reproducibility expressed in terms of the relative standard deviation (RSD) was about 3.8% (n=5) at a CEA concentration of 3.0 ng ml^{-1}, indicating a good reproducibility of the proposed immunosensor.

In order to assess the selectivity of the immunosensor, interferences study was performed using bovine serum albumin (BSA), prostate specific antigen (PSA), horseradish peroxidase (HRP) and glucose. The 3.0 ng ml^{-1} of CEA solution containing 30.0 ng ml^{-1}

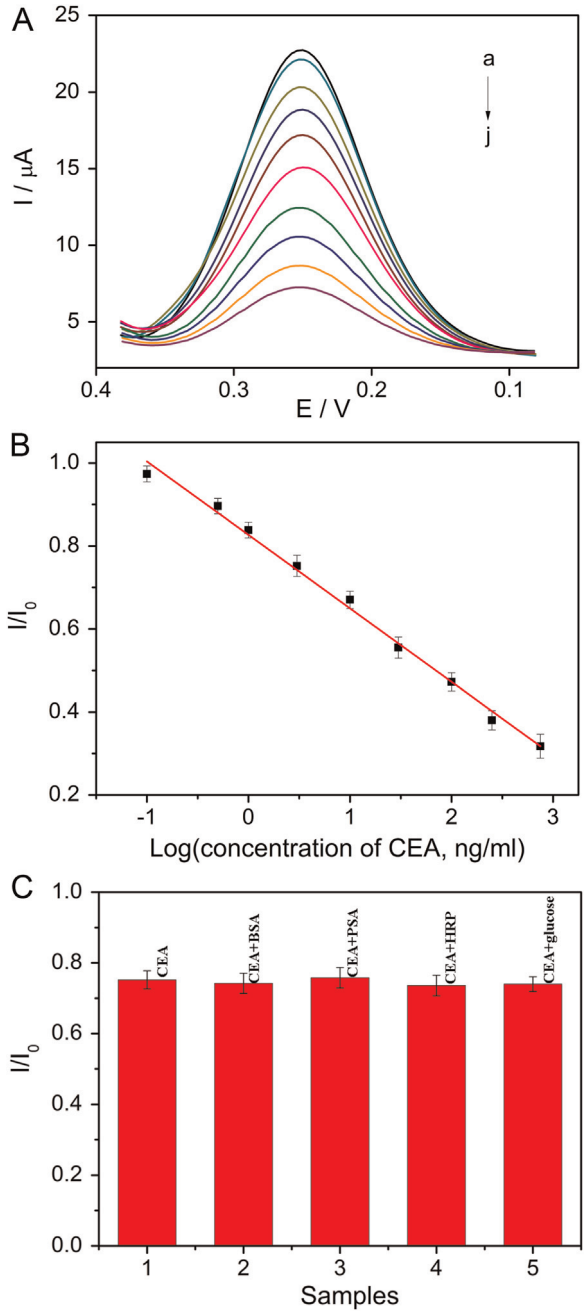

Fig. 6. (A) DPV responses of the immunosensor after being incubated in different concentrations of CEA: 0, 0.1, 0.5, 1.0, 3.0, 10.0, 30.0, 100.0, 250.0, 750.0 ng ml^{-1} (from a to j). (B) The calibration plot of I/I_0 versus the logarithm of CEA concentration under optimal conditions. Error bar=RSD (n=3). (C) Interference experiments for 3.0 ng ml^{-1} CEA (1), 3.0 ng ml^{-1} CEA within 30.0 ng ml^{-1} BSA (2), 3.0 ng ml^{-1} CEA within 30.0 ng ml^{-1} PSA (3), 3.0 ng ml^{-1} CEA within 30.0 ng ml^{-1} HRP (4), and 3.0 ng ml^{-1} CEA+30.0 ng ml^{-1} glucose (5). Error bar=RSD (n=3).

of interfering substances was measured by the immunosensor and the results were shown in Fig. 6C. The ratio variation due to the interferences was less than 3.4% of that without them, suggesting a high selectivity of the developed immunosensor.

The stability of the immunosensors was also examined by detecting periodically their DPV current responses to a 3.0 ng ml^{-1} of CEA solution. When not in use, the immunosensors were stored at 4 °C. After 3 weeks, the DPV response maintained almost 94% of its initial response. This further indicated that the prepared immunosensor provided a good biocompatible microenvironment

which was efficient for retaining the bioactivity and preventing the biomolecules from leaking out.

3.5. Real sample analysis

To examine the practical application of the proposed CEA immunosensor in serum sample, we performed recovery experiment in bovine serum matrix (1:20 diluted with 0.05 M phosphate buffer solution, pH 7.0). Though bovine serum contains a large variety of proteins and other biomolecules, very slight change was observed when the immunosensor was immersed in it for 30 min. DPV responses were obtained in various CEA (1.0, 3.0, 10.0 ng ml^{-1}) spiked serum samples. The CEA recovery was between 96% and 103% and the RSD was less than 3.2% ($n=3$) (Table S1 in Supplemental Information), which clearly indicated the potentiality of the present immunosensor for clinical detection of the CEA level in real serum samples. The highly selectivity can be attributed, at least in part, to the effective antibody immobilization mediated by lectin–sugarprotein interaction, which offers an indirect and oriented immobilization on biocompatible matrix. Combined with the macroporous morphology of 3D-G, antibodies can be immobilized onto the 3D electrode to provide high activity and excellent recognition ability.

4. Conclusion

In this study, we demonstrate the use of 3D-G foam as novel electrode architecture for immunosensing of tumor biomarker. The biosensor presents outstanding performance in terms of detection range, sensitivity, lower detection limit, and stability. Such excellent performance can be attributable to: (1) the macroporous structure of graphene foam which ensures efficient mass transport and accessibility of bioaffinity ligands; (2) large active surface area of 3D electrode which proves high density of the immobilized antibody; (3) high electrode conductivity due to extraordinary conductive nature of graphene and the 3D multiplexed conductive pathways of graphene foam; (4) the used indirect immobilization of antibody mediated by lectin–sugarprotein interaction avoids the destruction of activity and recognition ability; (5) DPV gives fast and sensitive detection. The proposed immunosensor can be applied for detecting other proteins by simply changing the respective antibodies and can be used as a versatile platform for reliable cancer diagnostics in clinical and biochemical analyses.

Acknowledgments

We acknowledge the financial support from the financial support from the National Natural Science Foundation of China (Nos. 21305127, 21190040, 11174105 and 91227114), the Science Foundation of Zhejiang Sci-Tech University (13062173-Y) and 521 talent project of ZSTU.

Appendix A. Supplementary material

Supplementary data associated with this article can be found in the online version at http://dx.doi.org/10.1016/j.bios.2014.10.016.

References

Begard, K., Abdollah, S., Rahman, H., Kamal, A., 2014. Biosens. Bioelectron. 52, 20–28.
Cai, Y., Li, H., Li, Y., Zhao, Y., Ma, Y., Ma, H., Zhu, B., Xu, C., Wei, Q., Wu, D., Du, B., 2012. Biosens. Bioelectron. 36, 6–11.
Chen, H., Tang, J., Su, B., Chen, G., Huang, J., Tang, D., 2010. Anal. Chim. Acta 678, 169–175.
Chen, Z., Ren, W., Gao, L., Liu, B., Pei, S., Cheng, H.M., 2011. Nat. Mater. 10, 424–428.
Cheng, C., Nie, S., Li, S., Peng, H., Yang, H., Ma, L., Sun, S., Zhao, C., 2013. J. Mater. Chem. B 1, 265–275.
Dong, X., Wang, X., Wang, L., Song, H., Zhang, H., Huang, W., Chen, P., 2012. ACS Appl. Mater. Interfaces 4, 3129–3133.
Dong, X., Xu, H., Wang, X., Huang, Y., Chan-Park, M., Zhang, H., Wang, L., Huang, W., Chen, P., 2012. ACS Nano 6, 3206–3213.
Du, D., Wang, L., Shao, Y., Wang, J., Engelhard, M.H., Lin, Y., 2011. Anal. Chem. 83, 746–752.
Feng, L., Chen, Y., Ren, J., Qu, X., 2011. Biomaterials 32, 2930–2937.
Fu, Z.F., Hao, C., Fei, X., Ju, H.X., 2006. J. Immunol. Methods 312, 61–67.
Fu, Z.F., Yan, F., Liu, H., Yang, Z.J., Ju, H.X., 2008. Biosens. Bioelectron. 23, 1063–1069.
Gao, X., Zhang, Y., Chen, H., Chen, Z., Lin, X., 2011a. Anal. Biochem. 414, 70–76.
Gao, X., Zhang, Y., Wu, Q., Chen, H., Chen, Z., Lin, X., 2011b. Talanta 85, 1980–1985.
Guo, S.J., Wen, D., Zhai, Y.M., Dong, S.J., Wang, E.K., 2011. Biosens. Bioelectron. 26, 3475–3481.
Huang, K.J., Niu, D.J., Xie, W.Z., Wang, W., 2010. Anal. Chim. Acta 659, 102–108.
Hu, S.H., Zhang, S.C., Hu, Z.C., Xing, Z., Zhang, X.R., 2007. Anal. Chem. 79, 923–929.
Jin, B., Wang, P., Mao, H., Hu, B., Zhang, H., Chen, Z., Wu, Z., Bian, X., Jia, C., Jing, F., Jin, Q., Zhao, J., 2014. Biosens. Bioelectron. 55, 464–469.
Kanso, H., Inguimbert, N., Barthelmebs, L., Istamboulie, G., Thomas, F., Calas-Blanchard, C., Noguer, T., 2014. Chem. Commun. 50, 1658–1661.
Kitano, H., 2002. Science 295, 1662–1664.
Lee, H., Dellatore, S., Miller, W., Messersmith, P., 2007. Science 318, 426–430.
Liu, J.Y., Qin, Y.N., Li, D., Wang, T.S., Liu, Y.Q., Wang, J., Wang, E.K., 2013. Biosens. Bioelectron. 41, 436–441.
Liu, Y., Dong, X.C., Chen, P., 2012. Chem. Soc. Rev. 41, 2283–2307.
Luo, X., Xu, Q., James, T., Davis, J.J., 2014. Anal. Chem. 86, 5553–5558.
Morris, T., Peterson, A., Tarlov, M., 2009. Anal. Chem. 81, 5413–5420.
Niederkofler, E.E., Tubbs, K.A., Gruber, K., Nedelkov, D., Kiernan, U.A., Williams, P., Nelson, R.W., 2001. Anal. Chem. 73, 3294–3299.
Ojeda, I., Garcinuño, B., Moreno-Guzmán, M., González-Cortés, A., Yudasaka, M., Iijima, S., Langa, F., Yáñez-Sedeño, P., Pingarrón, J.M., 2014. Anal. Chem. 86, 7749–7756.
Patel, J., Radhakrishnan, L., Zhao, B., Uppalapati, B., Daniels, R.C., Ward, K.R., Collinson, M.M., 2013. Anal. Chem. 85, 11610–11618.
Si, P., Dong, X.C., Chen, P., Kim, D.H., 2013. J. Mater. Chem. B 1, 110–115.
Srinivas, P.R., Kramer, B.S., Srivastava, S., 2001. Lancet Oncol. 2, 698–704.
Tang, J., Tang, D.P., Su, B.L., Li, Q.F., Qiu, B., Chen, G.N., 2011. Electrochim. Acta 56, 8168–8175.
Voller, A., Bartlett, A., Bidwell, D.E., 1978. J. Clin. Pathol. 31, 507–520.
Wang, L., Xu, M., Zhou, M., Han, L., Zhu, C., Dong, S., 2012. Anal. Chem. 84, 7301–7307.
Wang, L., Zhang, Q., Chen, S., Xu, F., Chen, S., Jia, J., Tan, H., Hou, H., Song, Y., 2014. Anal. Chem. 86, 1414–1421.
Xi, F.N., Zhao., D.J., Wang, X.W., Chen, P., 2013. Electrochem. Commun. 26, 81–84.
Xi, F.N., Gao, J.Q., Wang, J.E., Wang, Z.X., 2011. J. Electroanal. Chem. 656, 252–257.
Yang, T., Guan, Q., Li, Q., Meng, L., Wang, L., Liu, C., Jiao, K., 2013. J. Mater. Chem. B 1, 2926–2933.
Yates, A.M., Elvin, S.J., Williamson, D.E.J., 1999. Immunoassay 20, 31–44.
Zhang, B., Tang, D., Liu, B., Chen, H., Cui, Y., Chen, G., 2011. Biosens. Bioelectron. 28, 174–180.